Journal of Materials Science and Chemical Engineering, 2026, 14(3), 88-106
https://www.scirp.org/journal/msce
ISSN Online: 2327-6053
ISSN Print: 2327-6045

Fabrication of Optically Active Cerium Metal-Organic Framework (Ce-5AIA) for Photocatalytic Degradation of Remazol Brilliant Violet 5R (RBV-5R)

Aba Akebi Atta-Eyison[1*], Ruphino Zugle[2*]

[1]Industrial Laboratory Sciences Department, Faculty of Health and Allied Sciences, Takoradi Technical University, Takoradi, Ghana
[2]Department of Chemistry, School of Physical Sciences, College of Agriculture and Natural Sciences, University of Cape Coast, Cape Coast, Ghana
Email: *aba.atta-eyison@ttu.edu.gh, *rzugle@ucc.edu.gh

How to cite this paper: Atta-Eyison, A.A. and Zugle, R. (2026) Fabrication of Optically Active Cerium Metal-Organic Framework (Ce-5AIA) for Photocatalytic Degradation of Remazol Brilliant Violet 5R (RBV-5R). *Journal of Materials Science and Chemical Engineering*, **14**, 88-106.
https://doi.org/10.4236/msce.2026.143007

Received: January 10, 2026
Accepted: March 21, 2026
Published: March 24, 2026

Abstract

The potential of photocatalysis for degrading water pollutants has attracted considerable attention. This research aims to investigate the fabrication of an optical sensitive Cerium Metal-Organic Framework (Ce-5AIA) and its application in the photocatalytic degradation of Remazol Brilliant Violet 5R (RBV-5R). The primary objective is to assess the efficiency of the Cerium Metal-Organic Framework in environmental remediation. The Cerium Metal-Organic Framework was synthesized from cerium nitrate hexahydrate and 5-Aminoisophthalic acid using the solvothermal technique. Characterization tests, including Fourier transform infrared (FTIR), X-ray diffraction (XRD), scanning electron microscopy (SEM), and Thermogravimetric (TGA) analysis, were performed to confirm the successful formation and structural integrity of the synthesized Cerium Metal-Organic Framework. Characterization confirmed the successful synthesis and functionality of the Metal-Organic Framework as an effective catalyst. Synthesized Cerium Metal-Organic Framework was used for photocatalytic degradation of Remazol Brilliant Violet 5R (RBV-5R) as a sample pollutant under solar radiation. The photocatalytic degradation results indicated that the fabricated Cerium Metal-Organic Framework demonstrated significant photocatalytic degradation activity under solar radiation by effectively degrading Remazol Brilliant Violet 5R (RBV-5R). Stability study of the Cerium Metal-Organic Framework for photocatalytic activity indicated that the synthesized MOF was stable after four consecutive uses. These findings suggest that Cerium Metal-Organic Frameworks could serve as a sustainable and efficient solution for the

degradation of organic pollutants in aquatic environments.

Keywords

Cerium Metal-Organic Framework, 5-Aminoisophthalic Acid, Remazol Brilliant Violet 5R (RBV-5R), Photocatalysis, Solar Radiation, Degradation

1. Introduction

The increasing pollution of water bodies has become a critical environmental concern, necessitating innovative and sustainable methods for the degradation of hazardous pollutants. Among various water contaminants, synthetic dyes pose significant risks due to their toxic properties, resistance to biodegradation, and potential accumulation in aquatic ecosystems [1]-[3]. Remazol Brilliant Violet 5R (RBV-5R), a widely used textile dye, is particularly concerning due to its structural complexity and environmental persistence [4] [5]. As global awareness and regulations regarding water quality escalate, advanced remediation strategies are urgently needed to address these pollutants effectively.

Recent advancements in material science have highlighted the potential of Metal-Organic Frameworks (MOFs) as novel materials for environmental remediation. MOFs are crystalline, porous compounds made up of metal ions coordinated to organic ligands, and they exhibit high surface areas, tunable porosity, and versatile chemical properties [6] [7]. These characteristics make them particularly attractive for various applications, including gas storage, sensing, and catalysis. Among the diverse range of MOFs, Cerium Metal-Organic Frameworks (Ce-MOFs) have gained attention due to their unique optical properties and catalytic activity, especially in photochemical reactions [8] [9].

Photocatalysis is an emerging technology that employs light energy to enhance the adsorption capabilities of materials, facilitating the breakdown of hazardous compounds [10] [11]. Ce-MOFs exhibit strong light absorption capabilities due to the presence of cerium ions, which can be excited under solar irradiation [8] [12]. This photonic character equips Ce-MOFs with the potential to act as effective agents in the degradation of pollutants under sunlight, hereby addressing both energy efficiency and pollutant removal.

The synthesis of Ce-MOFs involves the solvothermal method, which has proven to be effective in producing high-quality crystalline materials with well-defined structures [13] [14]. 5-Aminoisophthalic acid (H_2-5AIA), a derivative of isophthalic acid, serves as a versatile ligand in the synthesis of Metal-Organic Frameworks (MOFs) due to its unique structural and chemical properties. This ligand is characterized by its two carboxylic acid functional groups (-COOH) and one amino group (-NH_2), which provide multiple points of coordination to metal ions, facilitating the formation of stable frameworks. The amino group can participate in hydrogen bonding and electron donation, enhancing the stability and

functional properties of the resulting MOF. Additionally, the presence of the rigid aromatic ring contributes to the overall structural integrity of the framework [15]-[17]. Using cerium nitrate hexahydrate and 5-Aminoisophthalic acid as precursors, we can achieve a stable framework that not only supports the catalytic activity but also minimizes the leaching of metal ions into the environment.

This study aims to investigate the efficacy of Ce-5AIA in the photocatalytic degradation of Remazol Brilliant Violet 5R (RBV-5R), by thoroughly characterizing the synthesized material and assessing its stability and photocatalytic effectiveness under solar radiation. This research not only provides an innovative solution to dye pollution but also emphasizes the importance of developing stable, reusable materials in the quest for sustainable environmental remediation methods. Through this work, we aim to establish a foundation for future studies that can further exploit the unique properties of Ce-MOFs in tackling various environmental challenges.

2. Experimental

2.1. Materials

For this study, high-purity chemical compounds essential for the synthesis of Cerium Metal-Organic Framework (Ce-5AIA) and subsequent experiments were sourced. Cerium (III) nitrate hexahydrate ($Ce(NO_3)_3{\cdot}6H_2O$), with a purity of 99.9%, was procured from Central Drug House (P) Ltd in India. This compound serves as the primary source of cerium in our framework synthesis. 5-aminoisophthalic acid (H_2-5AIA) with 94% purity was obtained from Sigma Aldrich in China. This organic ligand plays a vital role in coordinating with the cerium ions, aiding in the formation of a stable and functional MOF structure. N, N-dimethylformamide (DMF), with a 99% purity level, was sourced from Daejung Chemicals and Metals Co., Ltd. in Korea. DMF serves as the solvent in our solvothermal synthesis process, effectively dissolving both the metal nitrate and organic ligand to ensure a uniform distribution of reactants, which is essential for optimal crystal growth during synthesis. Remazol Brilliant Violet 5R (RBV-5R), purchased from Sigma-Aldrich (Merck), has a purity of 95.0%. This compound was used as a model pollutant to assess the photoadsorptive degradation capabilities of the synthesized Cerium Metal-Organic Framework (Ce-5AIA). Its complex structure and resistance to biodegradation make it an ideal candidate for testing the effectiveness of our materials in degrading water pollutants.

2.2. Synthesis of Cerium Metal-Organic Framework

A combination of 0.866 g (2 mmol) of cerium nitrate hexahydrate and 0.181 g (1 mmol) of 5-aminoisophthalic acid was dissolved in 40 ml of N, N-Dimethylformamide (DMF) and placed in a 100 ml Teflon-lined autoclave [18] [19]. The autoclave was then heated in an oven at a constant temperature of 140˚C for 24 hours. After the heating period, the autoclave was allowed to cool to room temperature. The resulting product was filtered, washed three times with DMF, and

then dried in the oven at 120˚C for 2 hours, yielding a marble white powder.

2.3. Characterization

Several tests were conducted to characterize the synthesized Cerium Metal-Organic Framework and the organic linker. Functional groups were identified through Fourier transform infrared (FTIR) analysis with a Bruker Alpha Spectrometer. Crystallinity was assessed using an Empyrean X-ray Diffractometer. Surface morphology and elemental composition were analyzed using a ZEISS EVO MA 15 SEM-EDS. The thermal stability of the MOF was evaluated with the SDT Q600 V20.9 System in a nitrogen atmosphere.

2.4. Photocatalytic Degradation Activity of Synthesized Cerium Metal-Organic Framework (Ce-5AIA)

The optical activity of the synthesized Cerium MOF was studied on Remazol Brilliant Violet 5R (RBV-5R). For each activity, a 100 mL beaker containing 50 mL of sample pollutant solution and Ce-5AIA as catalyst was stirred in the dark for 30 minutes to achieve adsorption/desorption equilibrium and then under solar light at 20,000 lux intensity for increasing time at 20 min interval to 120 min. The solar light intensity was measured using the YF-170 Digital Light Meter. A 5 mL aliquot was drawn at each stipulated time to observe the photocatalytic degradation of RBV-5R by the Cerium MOF using a JENWAY 7315 Spectrophotometer. The RBV-5R photocatalytic degradation efficiency was calculated using Equation (1).

$$\text{Percentage Photocatalytic Degradation Efficiency} = \frac{Ci - Ct}{Ct} \times 100 \quad (1)$$

where C_i is the initial concentration of the dye at time (t) = 0 (g/L), and C_t is the concentration at a given time (g/L).

The intermediates during the photocatalytic degradation were identified to confirm the removal of RBV-5R from water using SHIMADZU GC-MS QP 2020 with all the necessary operational specifications adopted.

3. Result

3.1. Synthesized Cerium Metal-Organic Framework (Ce-5AIA)

Figure 1 shows the synthesized cerium-5-aminoisophthalic acid metal-organic framework (Ce-5AIA) before and after activation. A linen white precipitate (a) yielded a marble white coloured powder (b) after activation, having a percentage mass yield of 43.17%.

3.2. Characterization

3.2.1. Functional Group Characterization

A comparative analysis of the FTIR spectrum of 5-aminoisophthalic acid (H_2-5AIA) and that of the cerium (Ce) metal-organic frameworks (Ce-5AIA) formed using H_2-5AIA as an organic linker is shown in Figure 2. The broad band from 3500 cm^{-1} to 2220 cm^{-1} for H_2-5AIA indicates the presence of the hydroxyl group

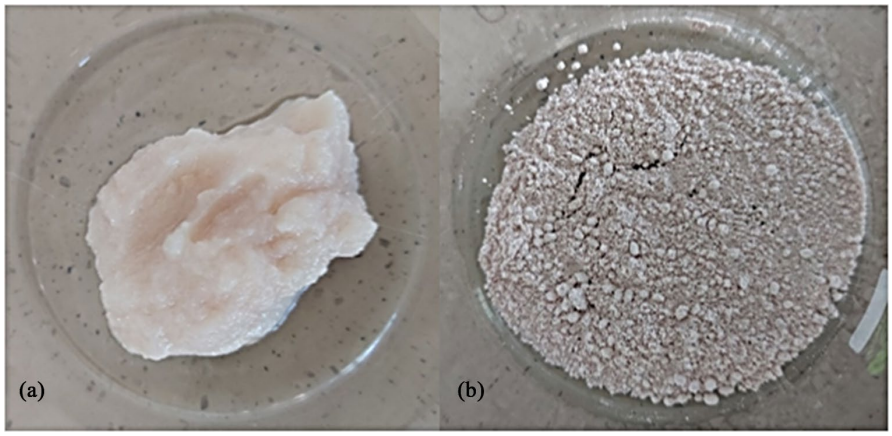

Figure 1. Images of synthesized Ce-5AIA (a) before activation, (b) after activation.

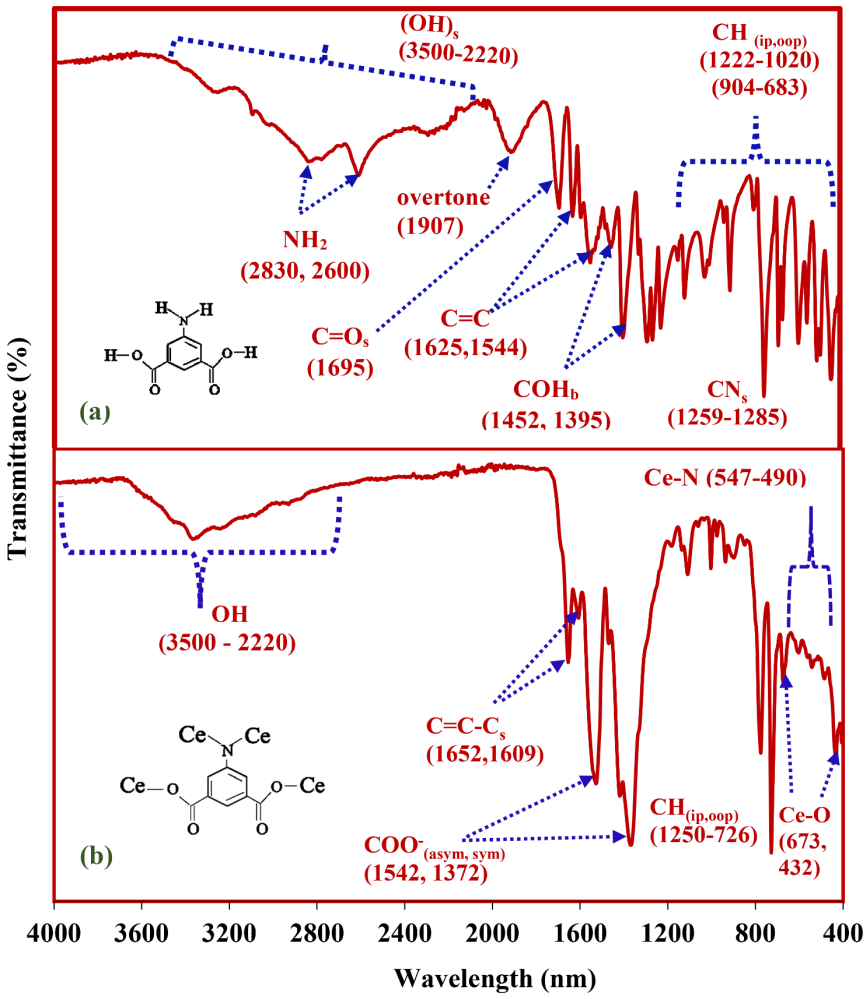

Figure 2. FTIR comparison of (a) 5-aminoisophthalic acid (H_2-5AIA) and (b) Synthesized Ce-MOF (Ce-5AIA).

(O-H) stretch typical of carboxylic acids [20]. The revealing double peaks within the broad band at 2830 cm^{-1} and 2600 cm^{-1} indicate the N-H stretch characteristic of primary aromatic amine. A shift of a broad band between 3650 cm^{-1} and 2862

$cm^{-1}$to the left, with the absence of double peaks observed for Ce-5AIA, depicts OH vibrational stretch due to water molecules adsorbed on the surface of Ce-5AIA from their metal hydrate salts, typical of most MOFs [21] [22]. The absence of a double band indicates the presence of a tertiary amine, which signifies a possible deprotonation of the primary amine to enable nitrogen (N) to form bonds with the Cerium (Ce). However, the absence of CN at around at 1285 cm^{-1} and 1258 cm^{-1} could be due to the overlap of the broad intense symmetric vibrational bands of COO- found around the region [20] [23]. The band at 1695 cm-1 for H_2-5AIA could be attributed to the presence of a C=O stretch carboxylic acid group [20] [24]. The bands observed between 1540 cm^{-1} and 1655 cm^{-1} indicate C=C-C stretching present in the aromatic ring of both Ce-5AIA and H_2-5AIA [23]. The bands detected at 1452 cm^{-1} and 1395 cm^{-1} for H_2-5AIA depict the bending of C-O-H [20] while strong absorption bands between 1542 cm^{-1} and 1372 cm^{-1} in the Ce-5AIA could be related to the asymmetric and symmetric vibrational modes of carboxylate (COO-) ions [22] [25]. The absence of COH in the synthesized MOFs indicates the deprotonation of COOH to yield COO^{-}, which can bond to the metals. The bands between 1220 cm^{-1} and 680 cm^{-1} found in both Ce-5AIA and H_2-5AIA are associated with the bending vibrational modes in the benzene ring. The bands from 1126 cm^{-1} to 930 cm^{-1} could relate to the in-plane C–H vibrational mode, while bands from 900 cm^{-1} to 680 cm^{-1} are out-of-plane vibrational modes [23].

The low-intensity stretching vibrational bands of Ce–O could be seen at 673 cm^{-1} and 432 cm^{-1} [18] while the very weak vibrational stretch of Ce-N could be observed from 547 cm^{-1} to 490 cm^{-1}. This is similar to metal-nitrogen (M-N) bond vibrations obtained in literature [26].

3.2.2. Crystallinity Characterization

The XRD pattern of the Ce-5AIA (b) in comparison with 5-Aminoisophthalic acid (H_2-5AIA) (a) is displayed in **Figure 3**. The diffractogram from 10˚ to 50˚ shows a 2θ peak pattern similar to the cerium-containing amine metal-organic frameworks reported [27].

The 2θ peaks at 16.13˚, 23.28˚, 28.56˚, 33.16˚, 41.07.44.59˚, and 47.79˚ were observed for Ce-5AIA (b), which were different peak patterns from those observed for H_2-5AIA. These peaks indicate that the Ce-5AIA is a crystalline compound and different from H_2-5AIA.

3.2.3. Morphology Characterization

The SEM-EDS image of 5-aminoisophtalic acid (H_2-5AIA) and synthesized Cerium metal-organic framework (Ce-5AIA) is shown in **Figure 4**. The SEM image of Ce-5AIA shows a rod-like rectangular prism shape morphology similar to other reported works related to cerium MOFs [27]-[29].

The EDS spectrum of 5-aminoisophtalic acid (H_2-5AIA) revealed the presence of carbon (C), oxygen (O), and nitrogen (N) with atomic percentages of 57.31% for carbon, 31.66% for oxygen, and 11.03% for nitrogen. The EDS spectrum of

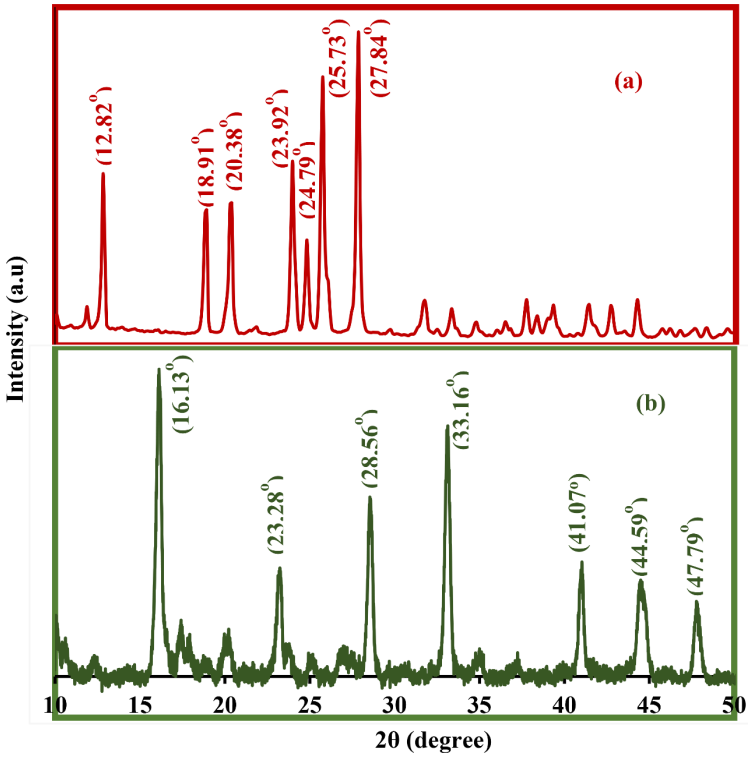

Figure 3. XRD of (a) 5-aminoisophthalic (H_2-5AIA) and (b) synthesized Ce-5AIA compound.

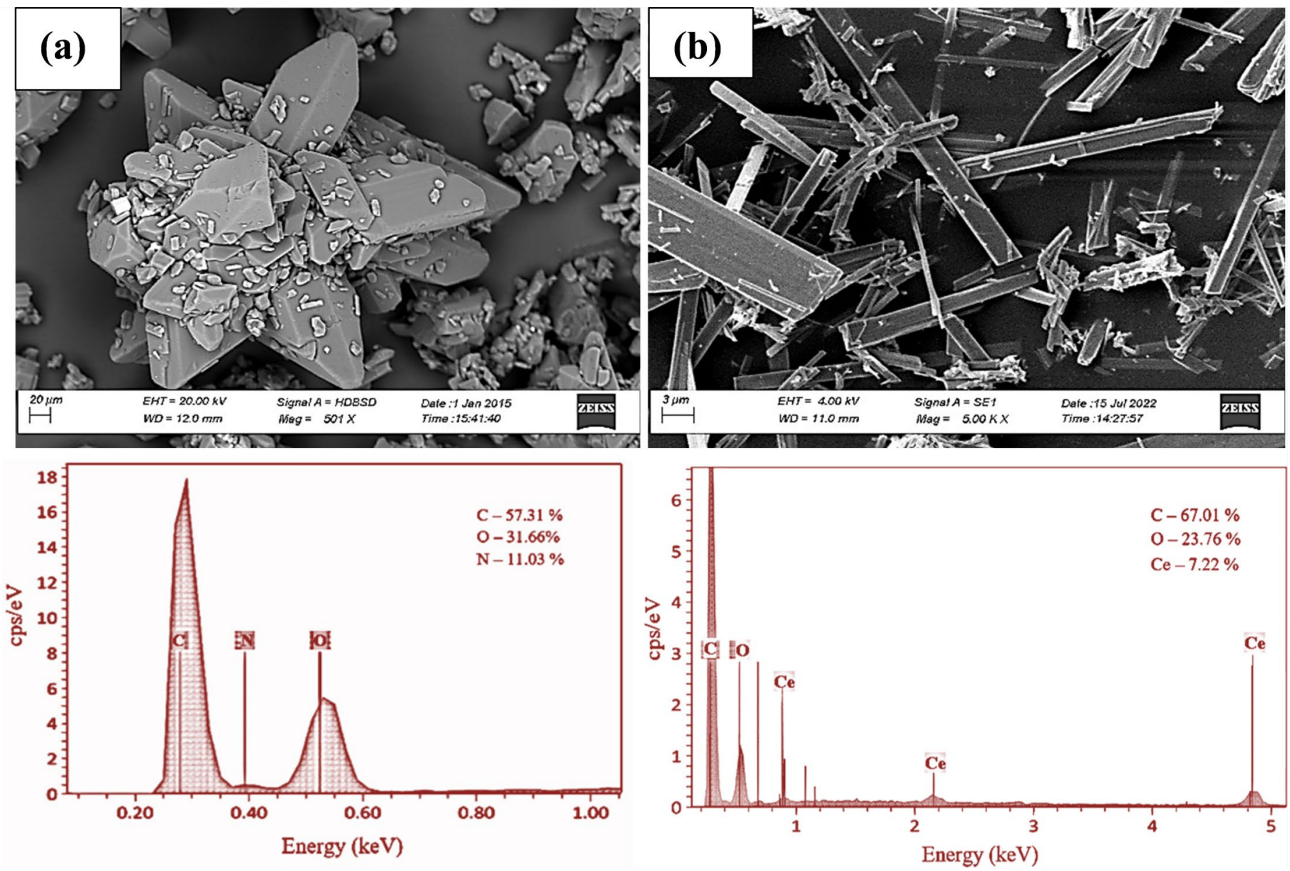

Figure 4. SEM-EDS of (a) 5-aminoisophthalic acid and (b) Ce-5AIA.

Ce-5AIA revealed the presence of carbon (C), cerium (Ce), and oxygen (O) with atomic percentages of 67.01% for carbon, 23.76% for oxygen, and 7.22% for cerium (Ce). Nitrogen was not identified from the EDS shown for the Ce-5AIA. The absence of nitrogen is due to an overlap of C and O k-alpha peaks, which are heavier than nitrogen and fall close to it [30]-[32]. Nitrogen (Kα at 0.392 keV) is a light element with a low atomic number (Z = 7). Its characteristic peak is located in the low-energy region of the EDS spectrum, specifically between the Kα peaks of Carbon (C, 0.277 keV) and Oxygen (O, 0.525 keV). Because EDS detectors have limited energy resolution, if the sample has high concentrations of Carbon and Oxygen, their intense peaks can overwhelm or obscure the much weaker Nitrogen peak. In many organic or oxidized materials, the Nitrogen(N) peak is hidden by the close proximity or overlap of C and O peaks, making it difficult to distinguish, especially if the nitrogen concentration is low. It is also possible that the nitrogen in the samples was absorbed by the beryllium window that separated the sample chamber from the analyzer during the EDS analysis [33].

3.2.4. Thermal Stability Characterization

The thermogram for the decomposition of Ce-5AIA is shown in **Figure 5**. Three major weight losses were observed from 50˚C to 800˚C. The first and second weight loss percentages of 6.88% and 13.74%, with corresponding exothermic rates of change of weight losses of 0.12%/min and 0.09%/min observed between 50˚C and 350˚C indicates the removal of the absorbed water molecules and organic solvents present in the Ce-5AIA [34]. A large weight loss percentage of 42.69% with a corresponding broad exothermic rate of change of weight loss peak at 0.13%/min observed between 350˚C and 750˚C indicates the decomposition of the Ce-5AIA [35].

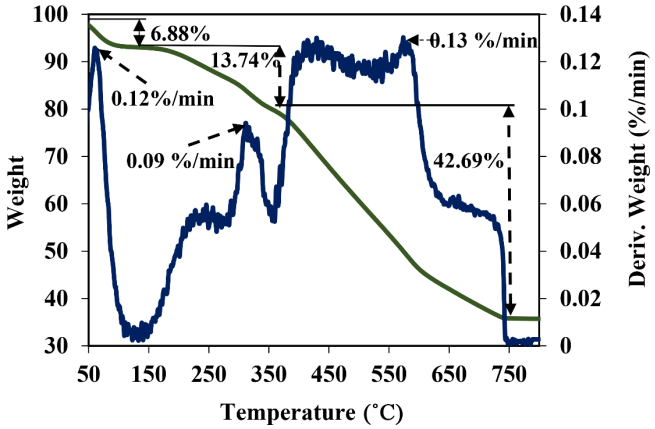

Figure 5. TGA-DSC of synthesized Ce-5AIA.

The decomposition could be due to the elimination of ligand molecules (-5AIA) as reported for other Ce MOF [19]. A slight weight loss from 750˚C to 800˚C confirms the formation of cerium oxide after the decomposition of the Ce-5AIA relative to literature [19] [36]. The decomposition of Ce-5AIA around 650˚C indi-

cates Ce-5AIA can withstand excessive heat and will only disintegrate above 600˚C.

3.3. Photocatalytic Degradation Activity of Synthesized Metal-Organic Framework on Pollutant

The photocatalytic degradation ability of Ce-5AIA on Remazol Brilliant Violet 5R (RBV-5R) is shown in Figure 6. Over 90% RBV-5R removal by Ce-5AIA was observed under solar irradiation after 120 min. Unappreciable degradation of RBV-5R was observed for both activity in the dark, with Ce-5AIA as a control experiment, and in the solar, without Ce-5AIA. A little over 5% result was observed throughout the experiment in the dark. This percentage is largely due to the adsorption/desorption activity of RBV-5R onto the surfaces of Ce-5AIA. A slightly lower percentage, marginally higher than 1%, was observed for the experiment under solar conditions without Ce-5AIA.

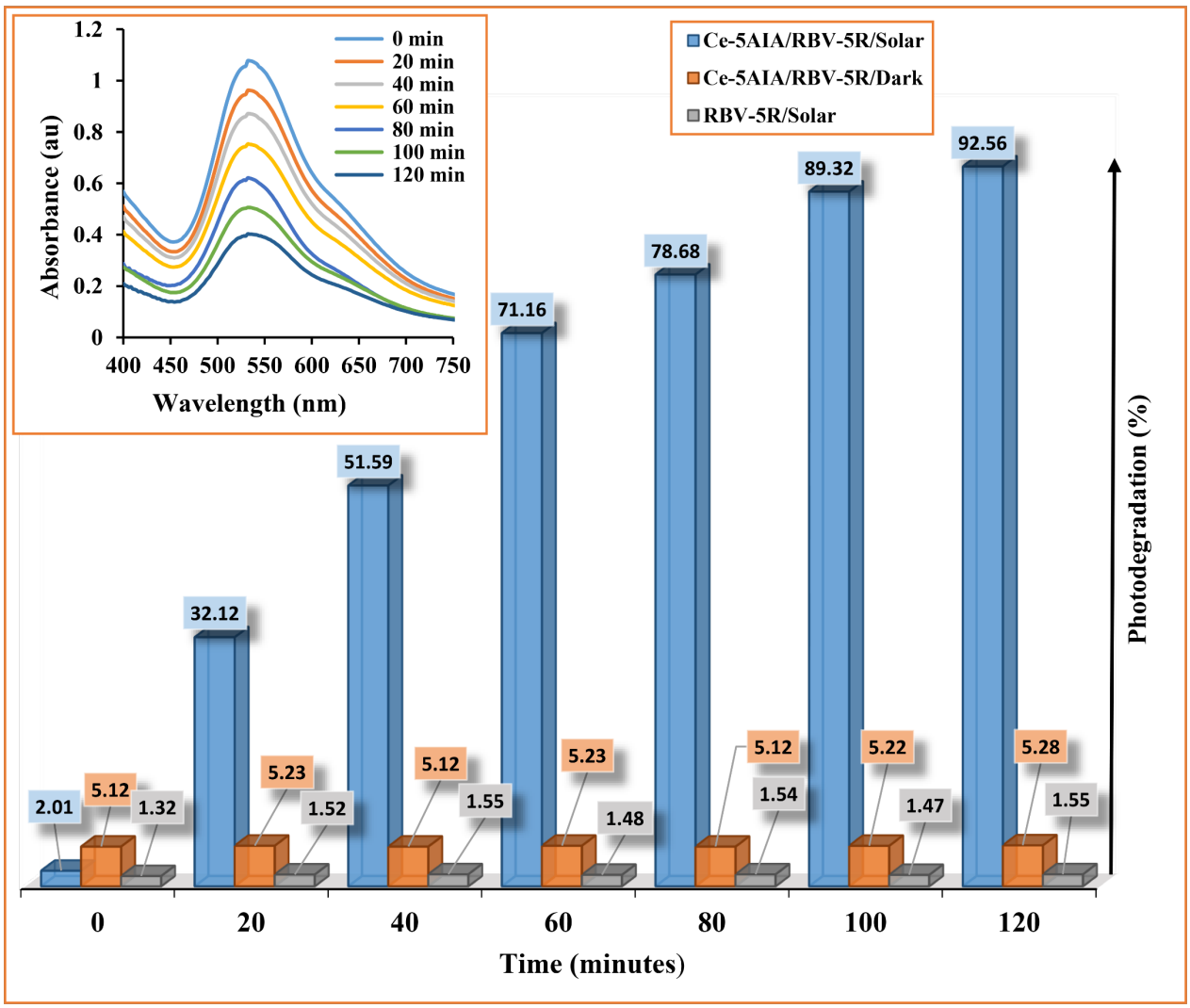

Figure 6. Photocatalytic activity of Ce-5AIA (Optimum parameters: [RBV-5R] = 0.30 g/L; Ce-5AIA Loading = 0.15 g/L; Solution pH = 6.2).

The UV-visible absorption spectrum of RBV-5R confirms a gradual reduction of peaks at 20 min time intervals over the 120 min, indicating RBV-5R's gradual removal from the sample solution.

3.4. Remazol Brilliant Violet 5R Concentration Variation Test

Figure 7 indicates the variation of Remazol Brilliant Violet 5R (RBV-5R) concentration with constant Ce-5AIA load to observe an optimum concentration for the photocatalytic degradation activity. An increase in photocatalytic degradation activity was observed with decreasing concentration of the RBV-5R.

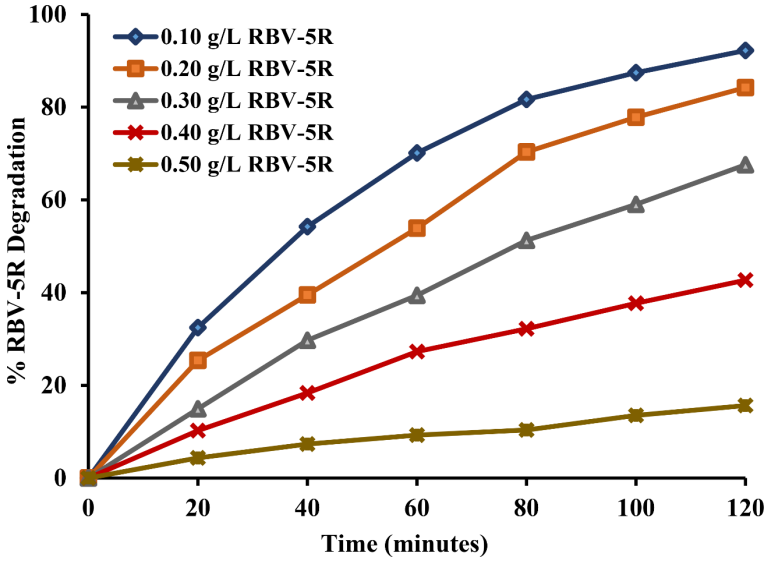

Figure 7. Effect of RBV-5R concentration variation on Ce-5AIA (Catalyst loading = 0.20 g/L; Solution pH = 6.2).

This decrease in photocatalytic degradation activity with an increase in concentration may be a result of the insufficient generation of photocatalytic radicals, such as ·OH, due to excess RBV-5R in solution, which may cover the active sites on MOFs, limiting the surface generation of ·OH radicals during photolysis. High RBV-5R concentration may also prevent a sufficient amount of light radiation from reaching the surfaces of the Ce MOF by absorbing a substantial amount of the radiation [10] [37]. This may reduce the photo-oxidation process. A concentration of 0.10 g/L RBV-5R was chosen as the optimum concentration for the photoadsorptive degradation, with over 80% degradation of RBV-5R reached after 120 minutes.

3.5. Cerium Metal-Organic Framework (Ce-5AIA) Amount Variation Test

Figure 8 shows the variation in the amount of Ce-5AIA with constant RBV-5R concentration to investigate their effect on the removal of RBV-5R. Lower RBV-5R removal was generally observed when the RBV-5R amount was decreased from 0.2 g/L to 0.05 g/L. The high pollutant removal efficiency for higher RBV-5R

amount may be due to an increase in available active sites to enhance the removal of RBV-5R [11] [38].

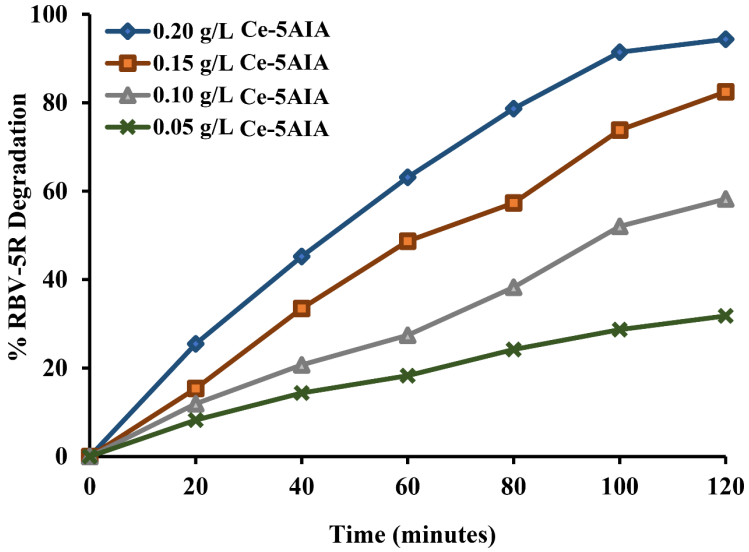

Figure 8. Effect of Ce-5AIA amount variation on the removal of Remazol Brilliant Violet 5R (RBV-5R) ([RBV-5R] = 0.10 g/L; Solution pH = 6.2).

Slow removal of the pollutants was observed when the amount of the Ce-5AIA was, however, observed between 100 min and 120 min for 0.20 g/L Ce-5AIA. The slow removal may be a result of the turbidity generated due to excess suspended MOF particles, which may limit the penetration of light radiation. An amount of the surface area of the Ce-5AIA may also be lost as a result of agglomeration [34] [35]. The 0.20 g/L Ce-5AIA amount was chosen as the optimum catalyst loading for the photocatalytic degradation of RBV-5R since over 90% of degradation was observed at 120 minutes.

3.6. Radical Scavenger Experiment

Figure 9 shows the photocatalytic degradation rate of RBV-5R solution with and without scroungers such as isopropanol (·OH scrounger), potassium iodide (h^+ scrounger), p-benzoquinone (O_2· scrounger), and silver nitrate (e^- scrounger).

The addition of isopropanol (·OH scrounger) showed a significant decrease in percentage degradation of 21.98% compared with potassium iodide (h^+ scrounger), p-benzoquinone ($O_2^{\cdot}$ scrounger), and silver nitrate (e^- scrounger), which showed very high percentage degradation of RBV-5R. The observed results reveal that the hydroxyl radical (·OH) is the primary operating radical during the photocatalytic degradation of RBV-5R.

3.7. Reusability of Cerium Metal-Organic Framework (Ce-5AIA) for the Degradation of Remazol Brilliant Violet 5R (RBV-5R)

Figure 10 shows a repetition of the photocatalytic degradation test for four series by reusing Ce-5AIA for the repeated test. The Ce-5AIA was relatively stable with

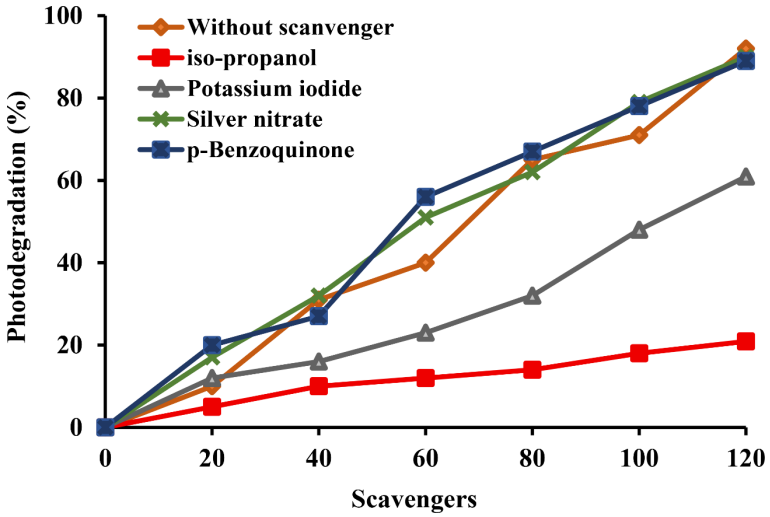

Figure 9. Photocatalytic degradation of Remazol Brilliant 5R (RBV-5R) with and without various scavengers under solar at120 min. ([RBV-5R] = 0.10 g/L, Ce-5AIA loading = 0.20 g/L; Solution pH = 6.2).

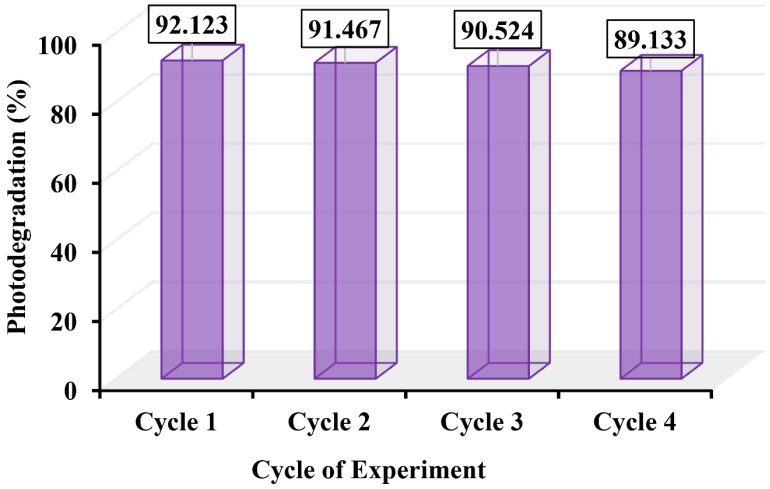

Figure 10. Reuse of Ce-5AIA for Repeated Photoadsorptive Degradation Test.

no considerable loss of activity for the repeated photocatalytic adsorptive activity on RBV-5R. This stability indicates its potential application for wastewater treatment.

The X-ray diffraction (XRD) result of Ce-5AIA before and after the cycle activity is shown in Figure 11. Similar diffraction peaks were observed after the cycle test, confirming the stability of RBV-5R.

3.8. GC-MS Analysis

Intermediates of RBV-5R during the photocatalytic degradation were monitored to understand the degradation profile of the process using the SHIMADZU GC-MS QP 2020. These Remazol Brilliant 5R (RBV-5R) with a molar mass of 734.58 g/mol were degraded into fragments shown in Figure 12. From Figure 12, higher and lower fragment intermediates were observed with strong peaks.

Intermediates observed are summarized in Table 1.

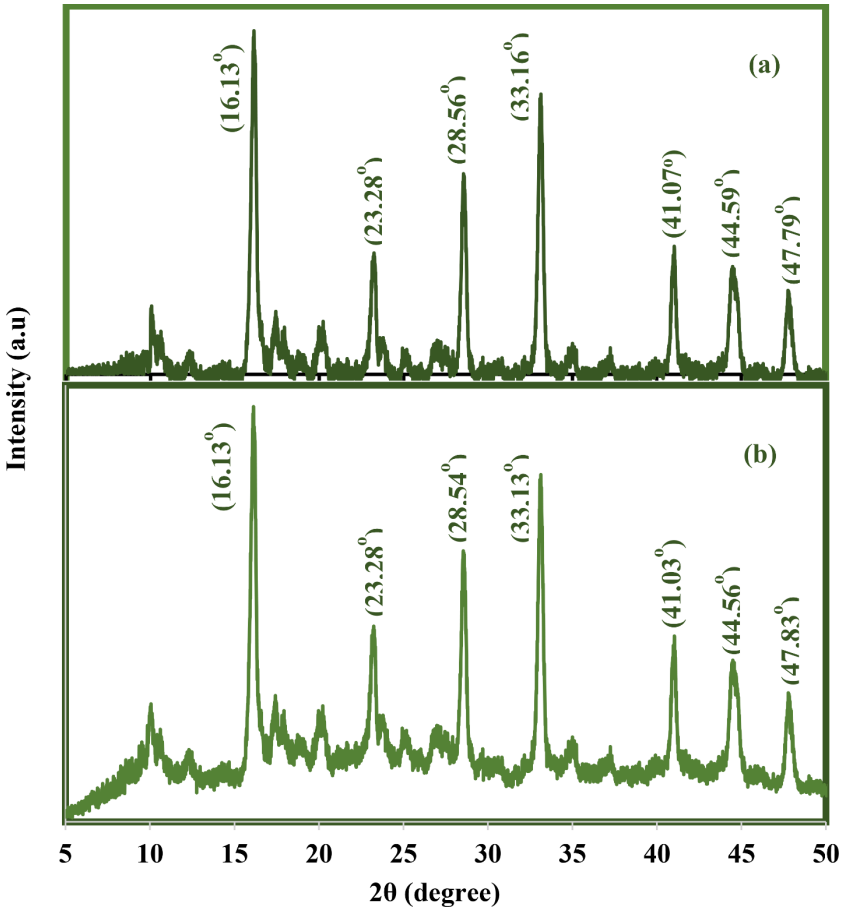

Figure 11. XRD of Ce-5AIA before (a) and after (b) Cycle photocatalytic degradation test.

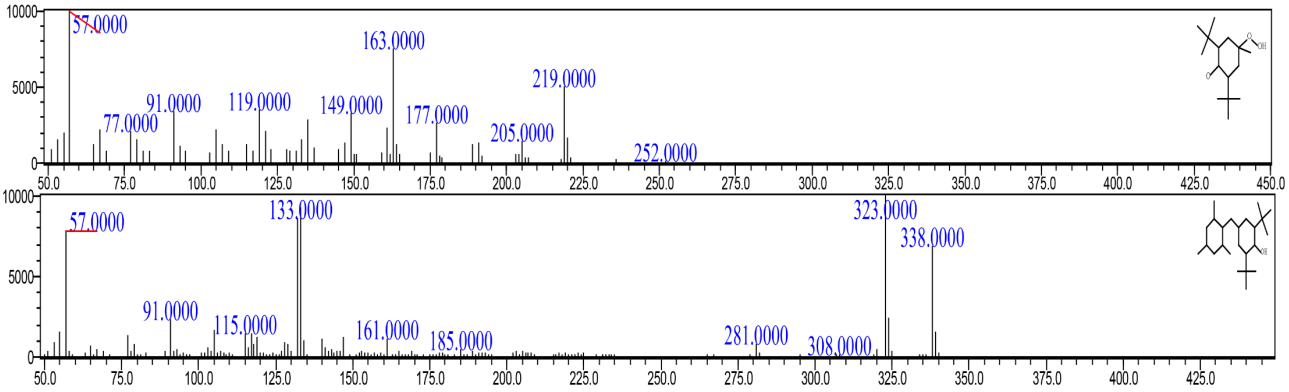

Figure 12. Mass spectroscopy of Pollutant after 120 min degradation by Ce-5AIA.

Higher intermediate fragments observed include Tetracosane (m/z 338), 4-Amino-5-hydroxy-2, 7-naphthalenedisulfonic (m/z 323), *N*-Phenyl-1-naphthylamine structure (m/z 219), Tryptophan (m/z 205), Diphenylamine 3-(m-nitrophenyl) sydnone (m/z 177), Phthalic acid (m/z 163), Ethyl benzoate (m/z 149), and Tyramine (m/z 133). Lower fragment intermediates observed include nitrobenzene (m/z119), 2-Heptylamine (m/z 115), Oxalic acid (m/z 91), Aniline (*m*/*z*

Table 1. Summary of Intermediates after 120 min Photocatalytic degradation of RBV-5R.

Pollutants	Intermediate			
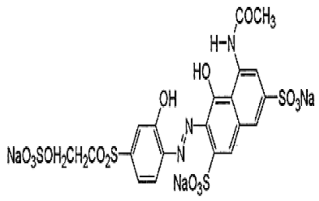 (734.58g/mol) Remazol brilliant violet 5R	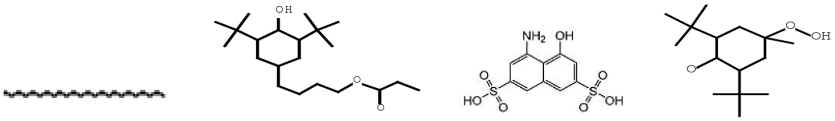 (338)	(m/z 332)	(m/z323)	(m/z 252)
	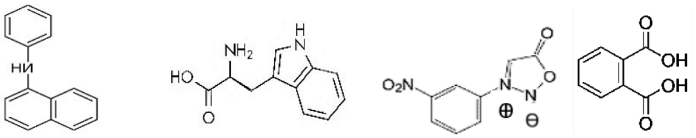 (m/z 219)	(m/z 205)	(m/z 177)	(m/z 163)
	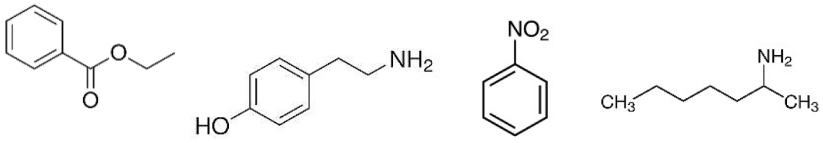 (m/z 149)	(m/z 133)	(m/z 119)	(m/z 115)
	 (m/z 91)	(m/z 91)	(m/z 77)	(m/z 57)

91), Phenyl ion (m/z77), and Acetic acid (m/z 57).

3.9. Proposed Degradation Pathway for Remazol Brilliant 5R (RBV-5R)

Based on the GC-MS analysis, a proposed degradation pathway diagram linking the identified intermediates could be achieved. Figure 13 shows the possible degradation pathway. Under high pressure or thermal conditions, Remazol Brilliant 5R (RBV-5R) fragments into larger species such as 4-Amino-5-hydroxy-2,7-naphthalenedisulfonic (m/z 323), N-Phenyl-1-naphthylamine (m/z 219), Tryptophan (m/z 205), Diphenylamine 3-(m-nitrophenyl) sydnone (m/z 177), Phthalic acid (m/z 163), Ethyl benzoate (m/z 149), and Tyramine (m/z 133). From the high molecular weight intermediates, various degradation pathways lead to lower molecular weight fragments. 4-Amino-5-hydroxy-2,7-naphthalenedisulfonic (m/z 323) and N-Phenyl-1-naphthylamine (m/z 219) degrades to produce 2-Heptylamine (m/z 115). N-Phenyl-1-naphthylamine (m/z 219) and Tryptophan (m/z 205) degrade to produce Nitrobenzene (m/z 119). Nitrobenzene (m/z 119) degrades further to produce Phenyl ion (m/z 77), which degrades to yield Acetic acid (m/z 57). Diphenylamine 3-(m-nitrophenyl) sydnone (m/z 177) degrades to produce Analine (m/z 91), which degrades further into Phenyl ion (m/z 77), which produces a lower fragment, Acetic acid (m/z 57). Phthalic acid (m/z 163), Ethyl benzoate (m/z 149), and Tyramine (m/z 133) degrade to produce Oxalic

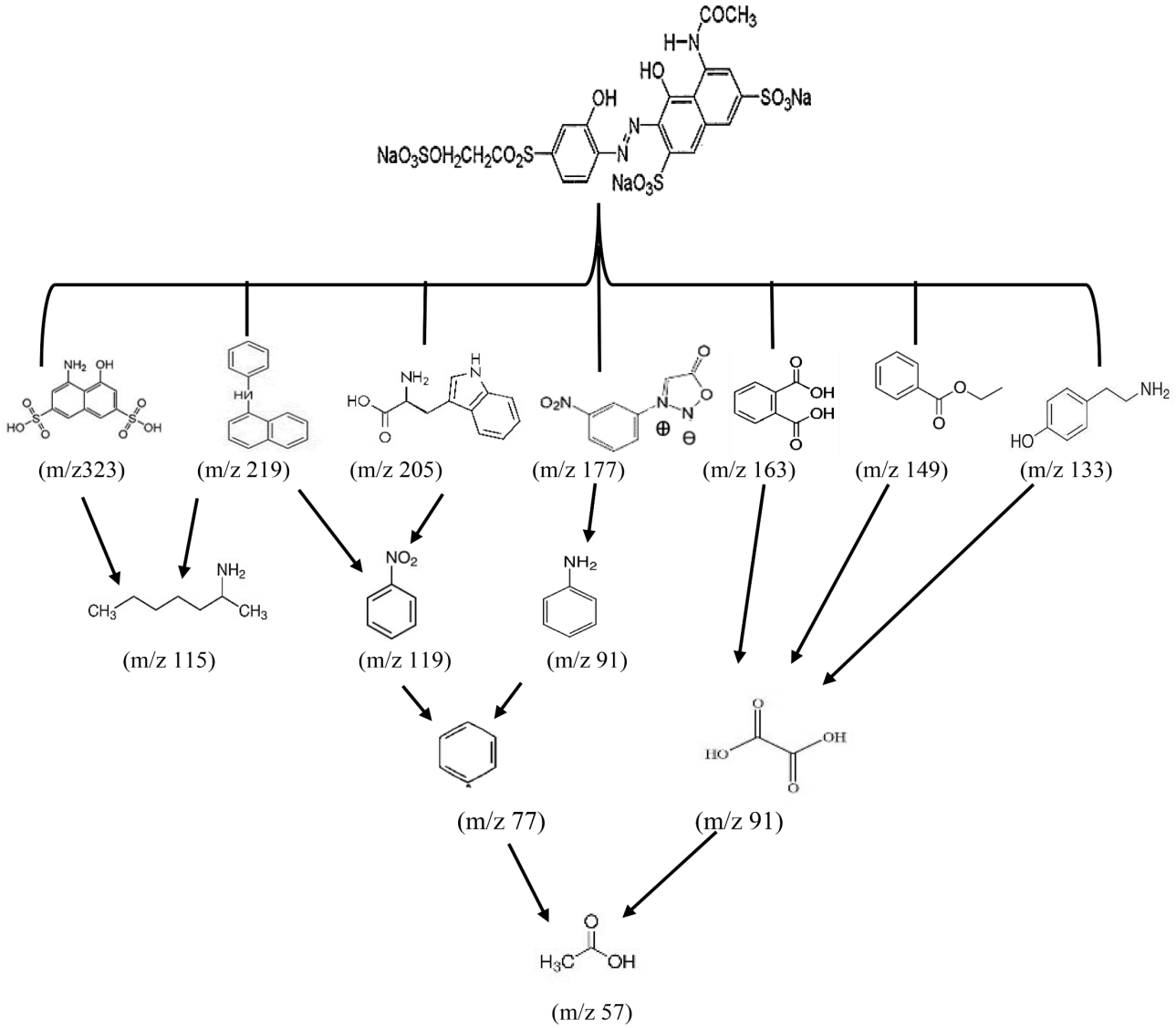

Figure 13. Proposed degradation mechanism for Remazol Brilliant 5R (RBV-5R).

acid (m/z 91), which further degrades to a lower fragment, Acetic acid (m/z 57).

4. Conclusions

This study successfully demonstrates the fabrication and application of an optically active Cerium Metal-Organic Framework (Ce-5AIA) for the photocatalytic degradation of Remazol Brilliant Violet 5R (RBV-5R), a persistent water pollutant. The synthesis of Ce-5AIA was achieved using a solvothermal method, producing a stable framework characterized by FTIR, XRD, SEM-EDS, and TGA analyses, which confirmed its structural integrity and functional properties. The Ce-5AIA exhibited significant photocatalytic activity, achieving over 90% degradation of RBV-5R under solar irradiation within 120 minutes. Stability tests indicated that the MOF retained its activity over multiple cycles, showcasing its potential for repeated use in wastewater treatment applications. The identification

of degradation intermediates through GC-MS confirmed the breakdown of RBV-5R into less harmful products, further validating the effectiveness of the Ce-5AIA in environmental remediation processes.

Overall, this research highlights the potential of Ce-MOFs as efficient and sustainable materials for tackling organic dye pollution in aquatic environments, paving the way for future studies that explore their application in other environmental challenges. The innovative approach of integrating photocatalysis with advanced materials science provides a promising pathway for developing cost-effective solutions to improve water quality and address environmental pollution.

Conflicts of Interest

The authors declare no conflicts of interest regarding the publication of this paper.

References

[1] Alsukaibi, A.K.D. (2022) Various Approaches for the Detoxification of Toxic Dyes in Wastewater. *Processes*, **10**, Article No. 1968. https://doi.org/10.3390/pr10101968

[2] Islam, T., Repon, M.R., Islam, T., Sarwar, Z. and Rahman, M.M. (2022) Impact of Textile Dyes on Health and Ecosystem: A Review of Structure, Causes, and Potential Solutions. *Environmental Science and Pollution Research*, **30**, 9207-9242. https://doi.org/10.1007/s11356-022-24398-3

[3] Kolya, H. and Kang, C. (2024) Toxicity of Metal Oxides, Dyes, and Dissolved Organic Matter in Water: Implications for the Environment and Human Health. *Toxics*, **12**, Article No. 111. https://doi.org/10.3390/toxics12020111

[4] Ismanto, A., Sukmono, Y., Hadibarata, T., Yeow, P.K., Indrayanti, E., Ismunarti, D.H., *et al.* (2023) Removal of Remazol Brilliant Blue R and Remazol Brilliant Violet 5r Dyes from Aqueous Solution by Adsorption Using Coffee Residue. *Environmental Quality Management*, **33**, 47-57. https://doi.org/10.1002/tqem.21983

[5] Lai, H.J. (2021) Adsorption of Remazol Brilliant Violet 5R (RBV-5R) and Remazol Brilliant Blue R (RBBR) from Aqueous Solution by Using Agriculture Waste. *Tropical Aquatic and Soil Pollution*, **1**, 11-23. https://doi.org/10.53623/tasp.v1i1.10

[6] Cai, G., Yan, P., Zhang, L., Zhou, H. and Jiang, H. (2021) Metal-Organic Framework-Based Hierarchically Porous Materials: Synthesis and Applications. *Chemical Reviews*, **121**, 12278-12326. https://doi.org/10.1021/acs.chemrev.1c00243

[7] Chakraborty, G., Park, I., Medishetty, R. and Vittal, J.J. (2021) Two-Dimensional Metal-Organic Framework Materials: Synthesis, Structures, Properties and Applications. *Chemical Reviews*, **121**, 3751-3891. https://doi.org/10.1021/acs.chemrev.0c01049

[8] Bhattacharyya, A., Gutiérrez, M., Cohen, B., Szalad, H., Albero, J., Garcia, H., *et al.* (2023) Unraveling the Optimal Cerium Content for Boosting the Photoresponse Activity of Mixed-Metal Zr/Ce-Based Metal-Organic Frameworks through a Photodynamic and Photocurrent Correlation: Implications on Water Splitting Efficiency. *ACS Applied Materials & Interfaces*, **15**, 36434-36446. https://doi.org/10.1021/acsami.3c08062

[9] Jacobsen, J., Ienco, A., D'Amato, R., Costantino, F. and Stock, N. (2020) The Chemistry of Ce-Based Metal-Organic Frameworks. *Dalton Transactions*, **49**, 16551-16586.

https://doi.org/10.1039/d0dt02813d

[10] Haleem, A., Shafiq, A., Chen, S. and Nazar, M. (2023) A Comprehensive Review on Adsorption, Photocatalytic and Chemical Degradation of Dyes and Nitro-Compounds over Different Kinds of Porous and Composite Materials. *Molecules*, **28**, Article No. 1081. https://doi.org/10.3390/molecules28031081

[11] Liu, J., Liang, L., Su, B., Wu, D., Zhang, Y., Wu, J., *et al.* (2024) Transformative Strategies in Photocatalyst Design: Merging Computational Methods and Deep Learning. *Journal of Materials Informatics*, **4**, 33. https://doi.org/10.20517/jmi.2024.48

[12] Zhang, L., Chen, L., Yan, G., Liang, R. and Ou, H. (2024) Post-Modification Engineering of Cerium Metal-Organic Frameworks for Efficient Visible Light-Driven Water Oxidation. *Rare Metals*, **43**, 5802-5812. https://doi.org/10.1007/s12598-024-02844-0

[13] Hu, Z., Wang, Y. and Zhao, D. (2021) The Chemistry and Applications of Hafnium and Cerium(IV) Metal-Organic Frameworks. *Chemical Society Reviews*, **50**, 4629-4683. https://doi.org/10.1039/d0cs00920b

[14] Rafiq, K., Sabir, M., Abid, M.Z. and Hussain, E. (2024) Unveiling the Scope and Perspectives of MOF-Derived Materials for Cutting-Edge Applications. *Nanoscale*, **16**, 16791-16837. https://doi.org/10.1039/d4nr02168a

[15] Huang, X. and Kong, J. (2025) Thiazolothiazole Based Functional Metal-Organic Frameworks. *CrystEngComm*, **27**, 2611-2622. https://doi.org/10.1039/d5ce00169b

[16] Kanan, S.M. and Malkawi, A. (2020) Recent Advances in Nanocomposite Luminescent Metal-Organic Framework Sensors for Detecting Metal Ions. *Comments on Inorganic Chemistry*, **41**, 1-66. https://doi.org/10.1080/02603594.2020.1805319

[17] Khan, A., Giri, M., Kalpna, Kumar, S.S. and Bansal, S. (2021) Zinc-Based Metal-Organic Framework for Heavy Metal Sensing. In: *Metal-Organic Frameworks for Environmental Sensing*, American Chemical Society, 177-201. https://doi.org/10.1021/bk-2021-1394.ch007

[18] Lin, A., Ibrahim, A.A., Arab, P., El-Kaderi, H.M. and El-Shall, M.S. (2017) Palladium Nanoparticles Supported on Ce-Metal-Organic Framework for Efficient CO Oxidation and Low-Temperature CO_2 Capture. *ACS Applied Materials & Interfaces*, **9**, 17961-17968. https://doi.org/10.1021/acsami.7b03555

[19] Santos, P.F. and Luz, P.P. (2020) Synthesis of a Ce-Based MOF-76 with High Yield: A Study of Reaction Parameters Based on a Factorial Design. *Journal of the Brazilian Chemical Society*, **31**, 566-573. https://doi.org/10.21577/0103-5053.20190218

[20] Nandiyanto, A.B.D., Ragadhita, R. and Fiandini, M. (2022) Interpretation of Fourier Transform Infrared Spectra (FTIR): A Practical Approach in the Polymer/Plastic Thermal Decomposition. *Indonesian Journal of Science and Technology*, **8**, 113-126. https://doi.org/10.17509/ijost.v8i1.53297

[21] Nivetha, R., Sajeev, A., Mary Paul, A., Gothandapani, K., Gnanasekar, S., Bhardwaj, P., *et al.* (2020) Cu Based Metal Organic Framework (Cu-Mof) for Electrocatalytic Hydrogen Evolution Reaction. *Materials Research Express*, **7**, Article ID: 114001. https://doi.org/10.1088/2053-1591/abb056

[22] Sangeetha, S. and Krishnamurthy, G. (2020) Electrochemical and Photocatalytic Applications of Ce-MOF. *Bulletin of Materials Science*, **43**, 1-10. https://doi.org/10.1007/s12034-020-02225-0

[23] Nandiyanto, A.B.D., Oktiani, R. and Ragadhita, R. (2019) How to Read and Interpret FTIR Spectroscope of Organic Material. *Indonesian Journal of Science and Technol-*

ogy, **4**, 97-118. https://doi.org/10.17509/ijost.v4i1.15806

[24] Segneanu, A. E., Gozescu, I., Dabici, A., Sfirloaga, P. and Szabadai, Z. (2012) Organic Compounds FT-IR Spectroscopy (Vol. 145). InTech.

[25] Zhang, Q., Chen, M., Zhong, L., Ye, Q., Jiang, S. and Huang, Z. (2018) Highly Effective Removal of Metal Cyanide Complexes and Recovery of Palladium Using Quaternary-Ammonium-Functionalized MOFs. *Molecules*, **23**, Article No. 2086. https://doi.org/10.3390/molecules23082086

[26] Nzikayel, S., Akpan, I.J. and Adams, E.C. (2017) Synthesis, FTIR and Electronic Spectra Studies of Metal (II) Complexes of Pyrazine-2-Carboxylic Acid Derivative. *Medicinal Chemistry*, **7**, 321-323. https://doi.org/10.4172/2161-0444.1000475

[27] Dong, W. and Huang, Y. (2019) CeO_2/C Nanowire Derived from a Cerium(III) Based Organic Framework as a Peroxidase Mimic for Colorimetric Sensing of Hydrogen Peroxide and for Enzymatic Sensing of Glucose. *Microchimica Acta*, **187**, Article No. 11. https://doi.org/10.1007/s00604-019-4032-2

[28] Ramachandran, R., Xuan, W., Zhao, C., Leng, X., Sun, D., Luo, D., *et al.* (2018) Enhanced Electrochemical Properties of Cerium Metal-Organic Framework Based Composite Electrodes for High-Performance Supercapacitor Application. *RSC Advances*, **8**, 3462-3469. https://doi.org/10.1039/c7ra12789h

[29] Xie, J., Mu, Z., Yan, B., Wang, J., Zhou, J. and Bai, L. (2021) An Electrochemical Aptasensor for Mycobacterium Tuberculosis ESAT-6 Antigen Detection Using Bimetallic Organic Framework. *Microchimica Acta*, **188**, 1-10. https://doi.org/10.1007/s00604-021-05058-8

[30] Tessier, F. (2018) Determining the Nitrogen Content in (Oxy)nitride Materials. *Materials*, **11**, Article No. 1331. https://doi.org/10.3390/ma11081331

[31] Oliwa, K., Efe, S., Figiela, B. and Korniejenko, K. (2025) Synergistic Effects of Glass and Flax Fibers Reinforced in Fly Ash Geopolymer Matrix. *Materials*, **19**, Article No. 102. https://doi.org/10.3390/ma19010102

[32] Atta-Eyison, A.A. and Zugle, R. (2025) Effect of Parameter Variation on the Coordination of 5-Amino Benzene-1, 3-Dicarboxylic Acid under the Solvothermal Technique for Catalytic Adsorption. *Results in Chemistry*, **15**, Article ID: 102169. https://doi.org/10.1016/j.rechem.2025.102169

[33] McCormack, M.A., McFee, W.E., Whitehead, H.R., Piwetz, S. and Dutton, J. (2021) Exploring the Use of SEM-EDS Analysis to Measure the Distribution of Major, Minor, and Trace Elements in Bottlenose Dolphin (*Tursiops truncatus*) Teeth. *Biological Trace Element Research*, **200**, 2147-2159. https://doi.org/10.1007/s12011-021-02809-9

[34] Zheng, J., Wang, Z., Chen, Z. and Zuo, S. (2021) Mechanism of CeO_2 Synthesized by Thermal Decomposition of Ce-MOF and Its Performance of Benzene Catalytic Combustion. *Journal of Rare Earths*, **39**, 790-796. https://doi.org/10.1016/j.jre.2020.08.009

[35] Saadatkhah, N., Carillo Garcia, A., Ackermann, S., Leclerc, P., Latifi, M., Samih, S., *et al.* (2019) Experimental Methods in Chemical Engineering: Thermogravimetric Analysis—TGA. *The Canadian Journal of Chemical Engineering*, **98**, 34-43. https://doi.org/10.1002/cjce.23673

[36] Zhang, J., Chen, L. and Yang, K. (2019) *In Situ* Synthesis of CuO Nanoparticles Decorated Hierarchical Ce-Metal-Organic Framework Nanocomposite for an Ultrasensitive Non-Enzymatic Glucose Sensor. *Ionics*, **25**, 4447-4457. https://doi.org/10.1007/s11581-019-02996-5

[37] Khan, M.S., Li, Y., Li, D., Qiu, J., Xu, X. and Yang, H.Y. (2023) A Review of Metal-organic Framework (MOF) Materials as an Effective Photocatalyst for Degradation of Organic Pollutants. *Nanoscale Advances*, **5**, 6318-6348. https://doi.org/10.1039/d3na00627a

[38] Yue, C., Chen, L., Zhang, H., Huang, J., Jiang, H., Li, H., *et al*. (2023) Metal-Organic Framework-Based Materials: Emerging High-Efficiency Catalysts for the Heterogeneous Photocatalytic Degradation of Pollutants in Water. *Environmental Science: Water Research & Technology*, **9**, 669-695. https://doi.org/10.1039/d2ew00784c